

Cobalt and iron modified activated carbons from renewable sources as catalysts in methanol decomposition: Effect of the precursor

I. Genova¹, B. Tsyntsarski¹, M. Dimitrov¹, D. Paneva², D. Kovacheva³, T. Budinova¹, R. Ivanova¹, I. Mitov², N. Petrov¹, T. Tsoncheva^{1*}

¹*Institute of Organic Chemistry with Centre of Phytochemistry, Bulgarian Academy of Sciences, Acad. G. Bonchev str., bl.9, 1113 Sofia, Bulgaria*

²*Institute of Catalysis, Bulgarian Academy of Sciences, Acad. G. Bonchev str., bl.11, 1113 Sofia, Bulgaria*

³*Institute of General and Inorganic Chemistry, Bulgarian Academy of Sciences, Acad. G. Bonchev str., bl.11, 1113 Sofia, Bulgaria*

Received April 24, 2014; Revised May 27, 2014

Dedicated to Acad. Dimiter Ivanov on the occasion of his 120th birth anniversary

Activated carbons, prepared from different biomass waste precursors, such as peach and olive stones, were modified with nanosized cobalt and iron species by incipient wetness impregnation technique. The obtained materials were characterized by nitrogen physisorption, XRD, UV–Vis, FTIR, TPR, Moessbauer spectroscopy and tested as catalysts in methanol decomposition to hydrogen and CO. Both modifications of the activated carbon obtained from peach stones show higher catalytic activity. Among them, the Co modification is more active and significantly more selective and it could be successfully used as a low-cost and efficient catalyst for methanol decomposition to hydrogen and CO.

Key words: iron and cobalt nanoparticles, activated carbon, methanol decomposition

INTRODUCTION

Methanol decomposition attracts growing interest due to the advantage of safe and efficient in situ production of hydrogen which can find application in gas turbines, fuel cells, vehicles and industry [1-7]. Also the high endothermic character of reaction allows recovering the waste heat from vehicle exhausted gases and industrial processes [1-7]. Low-cost, working at relatively low temperatures, highly active and selective catalyst for the decomposition reaction is essential for the utilization of this concept. Activated carbons (ACs) are used worldwide in a huge number of applications that goes from domestic to industrial uses, such as gas storage, removal of pollutants and odours, gas purification and separation, as catalysts or catalyst supports and in a number of medical uses [8,9]. Wood and stones from different lignocellulosic materials are the most used precursors for the production of ACs, but other agricultural by-products have also been investigated, such as date pits, palm shells, almond tree pruning, sugar cane bagasse, sunflower seed hull, olive and peach stones, lignin, coconut shell, cherry stone and rice straws amongst others [8-15]. Thus

obtained ACs possess very high specific surface areas and their pore size distributions can be varied from almost completely microporous to ones containing substantial amount of meso- and macropores as well [9]. Their textural characteristic makes ACs very suitable as catalyst hosts, especially when contain substantial amount of mesoporosity that can facilitate the transportation of reactants and products of a given catalytic reaction. To improve the catalytic activity of activated carbons, usually an active metal component is introduced in order to reduce reaction times and allow working at milder operating conditions [16]. Besides, nanosized Co particles display a wide range of interesting size-dependent structural, electrical, magnetic, and catalytic properties. It was reported [17] that cobalt containing catalysts represent high activity for Fischer-Tropsch synthesis and NO_x reduction [18]. Besides, catalysts based on iron oxide/activated carbon system were found promising in the organic compounds removal from aqueous solution [19], H₂S elimination [20], and NO_x reduction [21]. We have investigated highly active iron and cobalt containing catalysts supported on activated carbon obtained by waste coal treatment by-products for methanol decomposition [22]. We reported that the dispersion and the composition of the loaded metal

* To whom all correspondence should be sent:

E-mail: tsoncheva@orgchm.bas.bg

© 2014 Bulgarian Academy of Sciences, Union of Chemists in Bulgaria

phase depend significantly on the presence of support surface functional groups [22].

The aim of current paper is to elucidate the role of agriculture precursor and the textural properties of the obtained activated carbon support material on the state of the introduced cobalt and iron nanoparticles. XRD, Nitrogen physisorption, UV-Vis, FTIR, temperature programmed reduction with hydrogen (TPR) were used for the samples characterization. The catalytic behaviour of the obtained nanocomposite materials was tested in methanol decomposition to CO and hydrogen.

EXPERIMENTAL

Materials

Biomass based activated carbons were produced by one-step process of hydro-pyrolysis, which includes treatment of 15 g precursor (crushed peach stones and olive stones) with water steam at 1023 K for 1 h at atmospheric pressure, and a heating rate of 10°C/min, in a stainless steel vertical reactor placed in a tube furnace. The obtained activated carbon samples are denoted as PAC and OAC, respectively. Their modification with Fe and Co was performed by incipient wetness impregnation, using the corresponding nitrate precursors. The metal loading in all materials was 8 wt. %. The nitrate precursor decomposition was performed at 773 K for 6 h. The obtained supported samples are denoted as M/S, where M is Co or Fe and S is PAC or OAC.

Methods of characterization

The porous structure of all activated carbons was studied by nitrogen physisorption at 77 K on Micromeritics ASAP 2020 instrument. The amount of various acidic oxygen-containing functional groups was determined by Boehm method using aqueous solutions of NaHCO₃, Na₂CO₃, NaOH, and C₂H₅ONa according the procedure described in [23]. The amount of basic sites was determined with 0.05 N HCl according the procedure described in [24].

Powder X-ray diffraction patterns were collected within the range of 5.3 to 80° 2 θ on a Bruker D8 Advance diffractometer with Cu K α radiation and LynxEye detector. The average crystallite size was evaluated by using the Scherrer equation. The UV-Vis spectra were recorded on a Jasco V-650 UV-Vis spectrophotometer equipped with a diffuse reflectance unit. The IR spectra (KBr pellets) were recorded on a Bruker Vector 22 FTIR spectrometer

at a resolution of 1–2 cm⁻¹, accumulating 64–128 scans. The Moessbauer spectra were obtained in air at room temperature with a Wissel (Wissenschaftliche Elektronik GmbH, Germany) electromechanical spectrometer working in a constant acceleration mode. A ⁵⁷Co/Cr (activity \cong 10 mCi) source and α -Fe standard were used. The experimentally obtained spectra were fitted by the least square-method. The TPR/TG (temperature-programmed reduction/thermo-gravimetric) analyses were performed in a Setaram TG92 instrument in a flow of 50 vol % H₂ in Ar (100 cm³ min⁻¹) and a heating rate of 5 K/min⁻¹.

Catalytic investigation

Methanol conversion was carried out in a fixed bed flow reactor, and argon is being used as carrier gas (50 cm³min⁻¹). The methanol partial pressure was 1.57 kPa. The catalysts (0.055 g) were tested under conditions of a temperature-programmed regime within the range of 350–770 K with a heating rate of 1 Kmin⁻¹. On-line GC analysis was performed on HP 5890 apparatus equipped with flame ionization and thermo-conductivity detectors and a PLOT Q column. The absolute callibration method and carbon based material balance were used for the product yields elucidation. CO selectivity was calculated as X_{CO}/X_{tot}*100, where X_{CO} and X_{tot} are the yield of CO and the amount of converted methanol molecules.

RESULTS AND DISCUSSION

Supports characterization

XRD patterns of parent AC materials (Fig. 1a) represent broad peaks around 26° and 43° 2 θ which are generally assigned to the formation of crystalline carbonaceous structure. The results show that PAC sample is characterized with more ordered structure (more intense 100 hkl reflection at 43°) and higher degree of carbonization than OAC. The OAC XRD pattern also shows additional reflections around 29° and 31° due to small Ca₂CO₃ and NaCl impurities, respectively. The nitrogen adsorption isotherms of parent activated carbons are of type I/IV, according to the IUPAC classification, which is characteristic of materials with well developed micro-mesoporous structure (Fig. 1b). The calculated textural parameters (Table 1) reveal that the activated carbon obtained from the olive stones possesses higher specific surface area and larger portion of micropores.

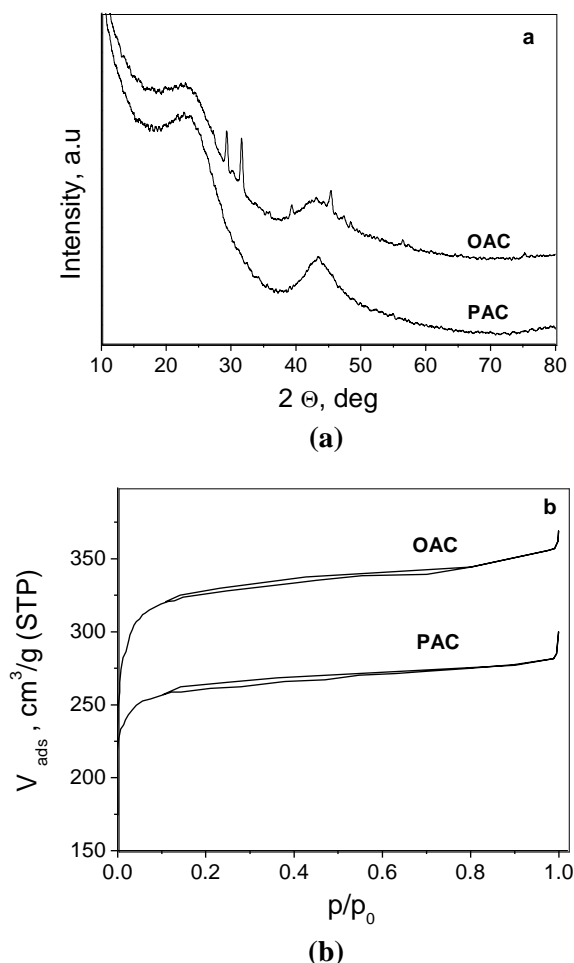


Fig. 1. Nitrogen physisorption isotherms (a) and XRD patterns (b) of pure AC materials.

The FTIR spectra of pure AC materials (not shown) display bands at $3000\text{--}2800\text{ cm}^{-1}$ that indicate the presence of aliphatic C–H stretching vibrations. Besides, the presence of bands at 1743 cm^{-1} and $1600\text{--}1500\text{ cm}^{-1}$ denotes the existence of carbonyl/carboxyl groups and an aromatic C=C ring stretching vibrations, respectively. More precise study of the accessible surface functional groups was performed by Boehm method. The experimental data show predominant presence of hydroxyl and carbonyl groups on both ACs, the latter being significantly more on OAC.

Both ACs represent almost similar amount of basic groups (Table 2).

Physicochemical characterization of Fe and Co modified activated carbons

The preservation of the isotherm shape after impregnation procedure reveals absence of structural collapse of ACs (Fig. 2a). The observed decrease in both BET surface area and total pore volume in comparison with the parent ACs could be assigned to the deposition of metal particles within the support pores or nearby pore openings (Table 1). The observed changes are more significant for OAC modified samples where predominant blocking of micropores could be assumed.

The XRD patterns of Fe/PAC and Fe/OAC (Fig. 2b) represent an intensive reflection at 35.4° and several smaller reflections at 30.5° , 43.5° , 57° , 62.9° 2θ which could be assigned to face-centered cubic (fcc) structure of Fe_3O_4 (PDF#19-0629) with average particle size of 11 and 19 nm, respectively. Intensive reflections at 36.5° , 42.2° and 61.4° 2θ in the XRD pattern of Co/PAC (Fig. 2b), indicate the presence of face centered (fcc) CoO phase (PDF#43-1004) with average particle size of 18 nm. New type of reflections, at 44.3° , 51.7° and 75.6° 2θ , belonging to cubic Co^0 phase (PDF#15-0806) with average particle size of 21 nm is registered for Co/OAC as well.

The FTIR spectra of the iron and cobalt modifications (not shown) display broad bands in the $600\text{--}500\text{ cm}^{-1}$ range, that could be assigned to the absorption of the Me–O bond in iron and cobalt oxide structures. The UV-Vis spectra of all modifications are presented in Fig. 3a. The absorption peaks are not well resolved. However, the slight absorption features with a maximum reflection at about $460\text{--}500\text{ nm}$ for the cobalt modifications could be carefully assigned to the presence of Co^{2+} ions in octahedral coordination and this is in accordance with the XRD data, where CoO was detected. The absorption above $400\text{--}500\text{ nm}$ for the

Table 1. Nitrogen physisorption data of the parent and modified activated carbons.

Sample	S_{BET} , [m ² /g]	V_{tot} , [cm ³ /g]	$V_{\text{mic}}(\text{DFT})$, [cm ³ /g]	$V_{\text{meso}}(\text{DFT})$, [cm ³ /g]	ΔS_{BET} , %	ΔV_{tot} , %
PAC	820	0.41	0.27	0.08		
OAC	910	0.63	0.33	0.09		
Fe/PAC	617	0.28	0.24	0.04	25	32
Fe/OAC	462	0.20	0.16	0.02	49	67
Co/PAC	655	0.28	0.20	0.04	20	30
Co/OAC	502	0.24	0.16	0.03	45	62

Table 2. Quantification of oxygen-containing groups on AC surface (meq/g).

Sample	Acid surface functional groups				Basic groups
	Carboxyl	Lactonic	Hydroxyl	Carbonyl	
PAC	BDL	BDL	0.29	1.07	1.04
OAC	BDL	BDL	0.21	1.69	1.19

BDL – below detection limits

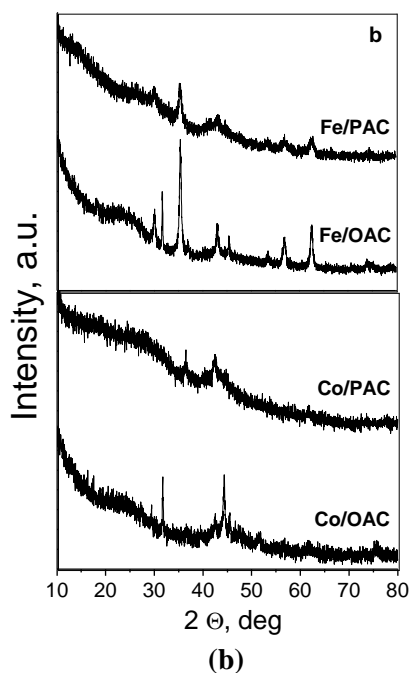
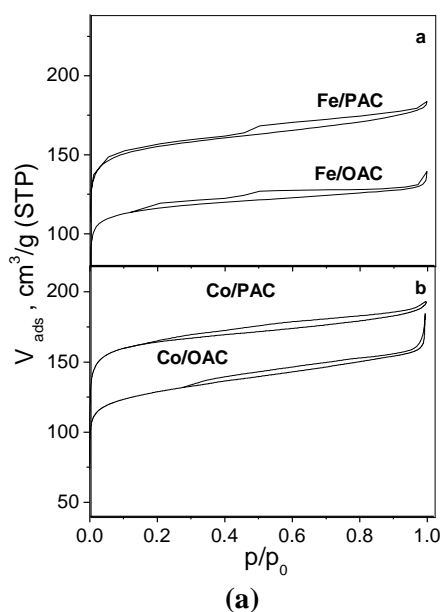


Fig. 2. Nitrogen physisorption isotherms with pore size distributions as insets (a) and XRD patterns (b) of iron and cobalt modified AC materials, respectively.

cobalt modifications could be carefully assigned to the presence of Co^{2+} ions in octahedral coordination and this is in accordance with the XRD data, where CoO was detected. The absorption above 400-500 nm in the spectra of iron modifications could be

assigned to $\text{Fe}^{n+} \leftarrow \text{O}^{2-}$ CT transitions in FeO_x particles.

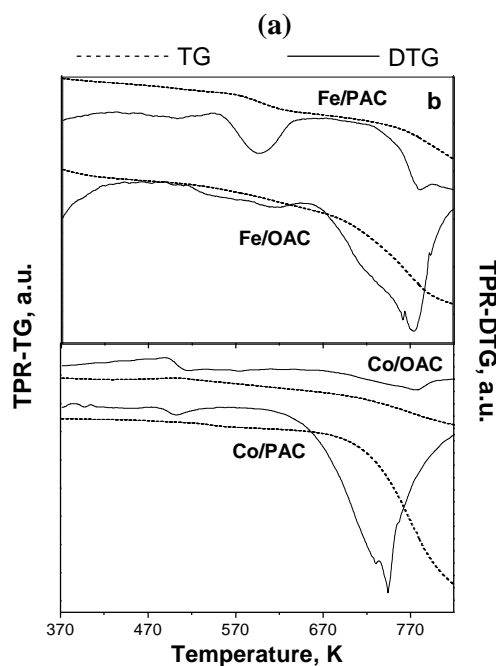
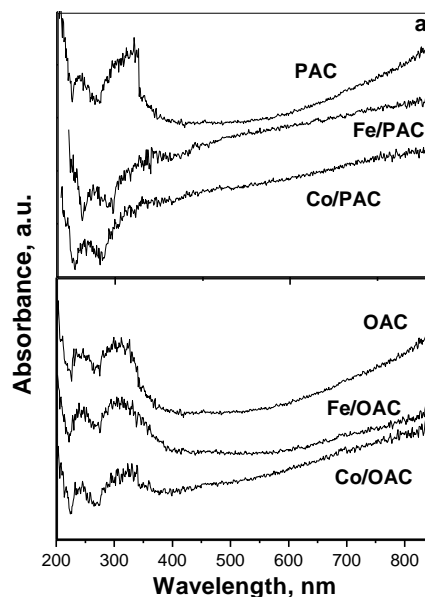


Fig. 3. UV-Vis spectra (a) and TPR data (b) of Fe- and Co- modified AC materials.

More information for the state of loaded iron species in the corresponding iron modifications is

Table 3. Moessbauer parameters of Fe/PAC and Fe/OAC samples before and after the catalytic test (*).

Sample	Components	IS, mm/s	QS, mm/s	Heff, T	FWHM, mm/s	G, %
Fe/PAC	Sx1- α -Fe ₂ O ₃	0.32	-0.10	49.8	0.50	3
	Sx2-Fe ₃ O ₄	0.30	0.01	47.6	0.42	10
	Sx3-Fe ₃ O ₄	0.64	0.01	43.7	1.35	61
	Db1-Fe ³⁺ _{octa} -SPM	0.34	0.72	-	0.52	12
	Db2-Fe ³⁺ _{octa} -SPM	0.31	1.05	-	0.73	14
Fe/OAC	Sx1-Fe ₃ O ₄	0.27	0.00	48.9	0.30	25
	Sx2-Fe ₃ O ₄	0.63	0.00	45.8	0.54	66
	Db1-Fe ³⁺ _{octa} -SPM	0.31	1.45	-	0.50	3
	Db2-Fe ³⁺ _{octa} -SPM	0.31	0.55	-	0.50	7
Fe/PAC*	Sx1-Fe ₃ O ₄	0.28	0.00	48.4	0.50	17
	Sx2-Fe ₃ O ₄	0.60	0.00	44.6	0.95	43
	Sx3-Fe ₃ C	0.20	0.02	20.5	0.69	19
	Db1-Fe ³⁺ _{octa} -SPM	0.35	0.58	-	0.45	10
	Db2-Fe ³⁺ _{octa} -SPM	0.35	1.02	-	0.58	11
Fe/OAC*	Sx1-Fe ₃ O ₄	0.29	0.00	48.2	0.50	5
	Sx2-Fe ₃ O ₄	0.65	0.00	45.1	0.75	7
	Sx3- α -Fe	0.00	0.00	33.2	0.28	39
	Sx4-Fe ₃ C	0.19	0.00	21.1	0.39	29
	Db1-Fe ²⁺ _{octa} -FeO	1.14	0.02	-	0.76	7
	Db2-Fe ³⁺ _{octa} -SPM	0.31	0.66	-	0.54	13

obtained by Moessbauer spectroscopy. The spectra of all iron modifications (not shown) are well fitted with sextets and doublets components. The calculated Moessbauer parameters (Table 3) of Fe/PAC show presence of hematite (Sx1- α -Fe₂O₃) particles with a relative weight of about 3%. The spectra of both iron samples consist mainly of sextets (Sx2 and Sx3) with parameters corresponding to highly dispersed magnetite phase with particle size below 30 nm and their relative weight is higher for Fe/OAC. The doublet part in the spectra reveals presence of ultra-dispersed iron oxide particles (up to 3-4 nm) with super paramagnetic (SPM) behaviour (Table 3).

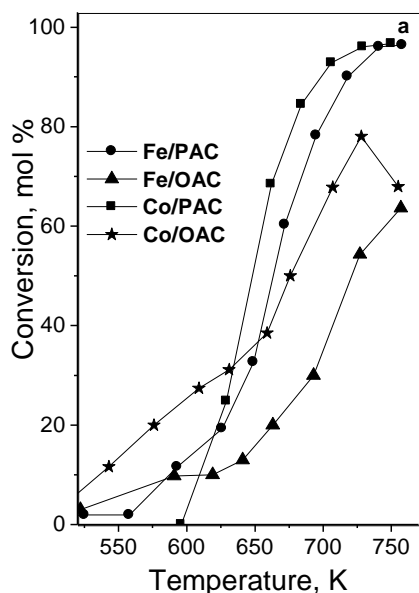
Additional information for the type and environment of metal ions was obtained by temperature programmed reduction with hydrogen (Fig. 3b). For the cobalt modifications, the observed effects up to 650 K could be assigned to the reduction to metallic cobalt of a mixture of Co₃O₄ and CoO species with different dispersion and location into the support porous structure [25]. In the case of Co/OAC, the reduction degree is smaller than the expected one. In accordance with XRD data this is due to the presence of substantial amount of metallic cobalt. Above 700 K, a significant weight loss was observed for both cobalt modifications that could be ascribed to the gasification of activated carbons promoted by the

presence of metallic Co, and this is much pronounced for the PAC modification.

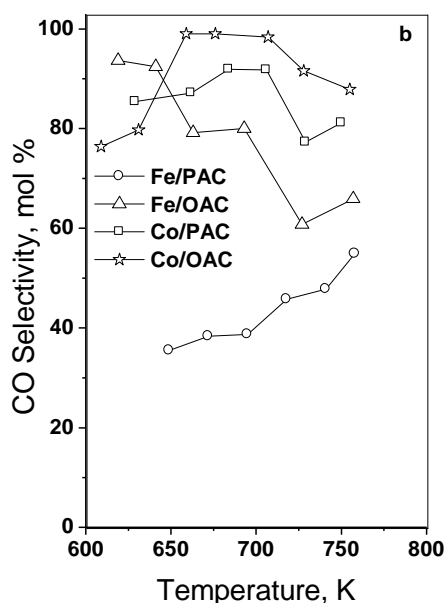
The TPR profiles for both iron modifications (Fig. 3b) represent broad reduction effect in the range of 400-650 K, which in accordance with XRD and Moessbauer data can be predominantly ascribed to step-wise reduction of Fe₃O₄ to FeO and then to Fe⁰. The TPR profile for Fe/OAC is broader and slightly shifted to higher temperature. Taking into account Moessbauer and nitrogen physisorption data, this could be due to lower dispersion of Fe₃O₄ and/or due to blocking of iron oxide particles into the micropores of the support. The significant weight loss is registered for both iron modifications above 660 K, which could be ascribed to gasification of the activated carbon supports, and again this is more pronounced for Fe/PAC.

The temperature dependencies of methanol conversion and CO selectivity on all modifications are presented in Fig. 4. The pure AC samples do not show any catalytic activity, and hence the influence of the observed by XRD impurities could be neglected. Among the iron modifications, Fe/PAC exhibits higher catalytic activity but lower selectivity to CO (below 60%) due to the formation of methane and CO₂. The Moessbauer data of Fe/PAC after the catalytic test (Table 3) show disappearance of the hematite phase and a decrease in the relative weight of Fe₃O₄ with the formation

of Fe₃C instead. At the same time, the ultra-dispersed nanoparticles with SPM behaviour remain almost unchanged, indicating that the reduction transformations affect only the larger particles. More pronounced reduction transformations of magnetite particles to α -Fe and Fe₃C under the influence of the reaction medium were established for Fe/OAC (Table 3).



(a)



(b)

Fig. 4. Methanol conversion (a) and CO selectivity (b) vs temperature on Fe- and Co- modifications of PAC and OAC.

Appearance of new phase of FeO nanoparticles with SPM behaviour was also registered. So, the observed differences in the catalytic behaviour of iron modifications (Fig. 4b) reflects in a complex way by the variations in the initial state of loaded iron (dispersion, location) and the reductive changes with it under the reaction medium. Obviously, the more pronounced blocking of micropores in OAC by the loaded iron species renders difficult the accessibility to the reactant molecules, leading to lower catalytic activity. However the more pronounced reduction changes with the iron oxide phase for Co/OAC seems to increase the CO selectivity. Among cobalt modifications, Co/PAC exhibits increase in the catalytic activity in a narrow temperature range above 600 K up to about 100% (Fig. 4a) and formation mainly of H₂ and CO (Fig. 4b). At the same time, Co/OAC (Fig. 2b) facilitates the methanol conversion even below 500 K, which is probably related to the presence of active metallic Co phase. However, the conversion curve for this sample is smoother with a maximum at 720 K due to fast deactivation, and this could be assigned to partial blocking of active phase into the micropores.

CONCLUSION

Highly active catalysts for methanol decomposition were prepared by deposition of cobalt and iron nanoparticles on activated carbons, obtained from waste biomass precursors, such as peach and olive stones. The dispersion, oxidative state and location of loaded particles could be successfully controlled by the textural peculiarities of the AC matrix. The best catalytic activity and selectivity is observed for cobalt modified AC from peach shells and it could be successfully used as low-cost efficient catalyst for methanol decomposition to hydrogen and CO.

Acknowledgements: Financial support from BAS and Bulgarian National Science Fund at the Ministry of Education and Science under Project DFNI-E01/7/2012 is gratefully acknowledged.

REFERENCES

1. J. R. Croy, S. Mostafa, J. Liu, Y. Sohn, B. R. Cuenya, *Catal. Lett.*, **118**, 1 (2007).
2. G. A. Olah, *Catal. Lett.*, **93**, 1 (2004).
3. P. Mizsey, E. Newson, T. B. Truong, P. Hottinger, *Appl. Catal. B*, **213**, 233 (2001).

4. K. W. Park, D. S. Han, Y. E. Sung, *J. Power Sources*, **163**, 82 (2006).
5. M. Borasio, O. R. de la Fuente, G. Rupprechter, H. J. Freund, *J. Phys. Chem. B*, **109**, 17791 (2005).
6. H. Borchert, B. Jurgens, T. Nowitzki, P. Behrend, Y. Borchert, V. Zielasek, S. Giorgio, C. R. Henry, M. Baumer, *J. Catal.*, **256**, 24 (2008).
7. J. C. Brown, E. Gulari, *Catal. Commun.*, **5**, 431 (2004).
8. K. Y. Foo, B. H. Hameed, *Chem. Eng. J.*, **184**, 57 (2012).
9. T. Budinova, D. Savova, B. Tsintsarski, C. O. Ania, B. Cabal, J. B. Parra, N. Petrov, *Appl. Surf. Sci.*, **255**, 4650 (2009).
10. W. Li, L. B. Zhang, J. H. Peng, N. Li, X. Y. Zhu, *Ind. Crop. Prod.*, **27**, 341 (2008).
11. J. Gñán, J. F. González, C. M. González-García, A. Ramiro, E. Sabio, S. Román, *Appl. Surf. Sci.*, **252**, 5993 (2006).
12. M. Olivares-Marín, C. Fernández-González, A. Macías-García, V. Gómez-Serrano, *Appl. Surf. Sci.*, **252**, 5967 (2006).
13. S. Guo, J. Peng, W. Li, K. Yang, L. Zhang, S. Zhang, H. Xia, *Appl. Surf. Sci.*, **255**, 8443 (2009).
14. W. C. Lim, C. Srinivasakannan, N. Balasubramanian, *J. Anal. Appl. Pyrolysis* **88**, 181 (2010).
15. I. I. Gurten, M. Ozmak, E. Yagmur, Z. Aktas, *Biomass Bioenergy*, **37**, 73 (2002).
16. A. Quintanilla, J. A. Casas, J. J. Rodríguez, *Appl. Catal. B*, **76**, 135 (2007).
17. M. Arsalanfar, A. A. Mirzaei, H. R. Bozorgzadeh, H. Atashi, S. Shahriari, A. Pourdolat, *J. Nat. Gas Sci. Eng.*, **9**, 119 (2012).
18. Z. H. Zhu, L. R. Radovic, G. Q. Lu, *Carbon*, **38**, 451 (2000).
19. M. H. Do, N. H. Phan, T. D. Nguyen, T. T. S. Pham, V. Nguyen, T. T. Vu, T. K. Nguyen, *Chemosphere*, **85**, 1269 (2011).
20. X. Yonghou, W. Shudong, W. Diyong, Y. Quan, *Separ. Pur. Tech.*, **59**, 326 (2008).
21. X. Gao, S. Liu, Y. Zhang, Z. Luo, K. Cen, *J. Hazard. Mater.*, **188**, 58 (2011).
22. T. Tsoncheva, I. Genova, B. Tsintsarski, M. Dimitrov, D. Paneva, Z. Cherkezova-Zheleva, T. Budinova, R. Ivanova, I. Mitov, N. Petrov, *J. Porous Mater.*, DOI: 10.1007/s10934-014-9797-4, in press.
23. H. P. Boehm, in: *Advances in Catalysis and Related Subjects*, D. D. Eley, H. Pines, P. B. Weisz (eds.), vol. 16, Academic Press, New York, 1966, p. 179.
24. E. Papier, S. Li, J. B. Donnet, *Carbon*, **25**, 243 (1987).
25. Y. Du, Q. Meng, J. Wang, J. Yan, H. Fan, Y. Liu, H. Dai, *Micropor. Mesopor. Mater.*, **162**, 199 (2012).

КАТАЛИЗАТОРИ ЗА РАЗЛАГАНЕ НА МЕТАНОЛ НА ОСНОВАТА НА КОБАЛТ И ЖЕЛЯЗО МОДИФИЦИРАН АКТИВЕН ВЪГЛЕН ОТ ВЪЗОБНОВЯЕМИ ИЗТОЧНИЦИ: ВЛИЯНИЕ НА ПРЕКУРСОРА

И. Генова¹, Б. Цинцарски¹, М. Димитров¹, Д. Панева², Д. Ковачева³, Т. Будинова¹, Р. Ивановна¹, И. Митов², Н. Петров¹, Т. Цончева^{1*}

¹ *Институт по органична химия с Център по фитохимия, Българска Академия на Науките, ул. Акад. Г. Бончев, бл. 9, 1113 София, България*

² *Институт по катализ, Българска Академия на Науките, ул. Акад. Г. Бончев, бл. 11, 1113 София, България*

³ *Институт по обща и неорганична химия, Българска Академия на Науките, ул. Акад. Г. Бончев, бл. 11, 1113 София, България*

Постъпила на 24 април 2014 г.; Коригирана на 27 май 2014 г.

(Резюме)

Два вида активен въглен, получени от различни прекурсори на основата на отпадъчна биомаса, съответно костилки от праскови и маслини, бяха модифициран с железни и кобалтови наночастици чрез импрегниране. Получените материали бяха охарактеризирани с помощта на физична адсорбция на азот, рентгенова дифракция (XRD), температурно-програмирана редукция с водород (TPR), UV-Vis, ИЧ- (FTIR) и Мьосбауерова спектроскопия и тествани като катализатори в реакция на разпадане на метанол до водород и СО. По-висока каталитична активност показаха модификациите на въглена, получен от прасковени костилки. Измежду тях, Со-съдържащият активен въглен е най-активен и значително по-селективен, и може с успех да бъде използван като евтин и ефективен катализатор в реакцията на разпадане на метанол до водород и СО.